Article

pubs.acs.org/Biomac

Acid-Activatable Prodrug Nanogels for Efficient Intracellular Doxorubicin Release

Fuxing Zhan,[†] Wei Chen,[†] Zhongjuan Wang,[‡] Wentao Lu,[†] Ru Cheng,[†] Chao Deng,[†] Fenghua Meng,[†] Haiyan Liu,[‡] and Zhiyuan Zhong*[,†]

[†]Biomedical Polymers Laboratory, and Jiangsu Key Laboratory of Advanced Functional Polymer Design and Application, Department of Polymer Science and Engineering, College of Chemistry, Chemical Engineering and Materials Science, Soochow University, Suzhou 215123, P. R. China

[‡]Laboratory of Cellular and Molecular Tumor Immunology, Institute of Biology and Medical Sciences, Soochow University, Suzhou 215123, P. R. China

ABSTRACT: Endosomal pH-activatable doxorubicin (DOX) prodrug nanogels were designed, prepared, and investigated for triggered intracellular drug release in cancer cells. DOX prodrugs with drug grafting contents of 3.9, 5.7, and 11.7 wt % (denoted as prodrugs **1**, **2**, and **3**, respectively) were conveniently obtained by sequential treatment of poly(ethylene glycol)-*b*-poly(2-hydroxyethyl methacrylate-*co*-ethyl glycinate methacrylamide) (PEG-*b*-P(HEMA-*co*-EGMA)) copolymers with hydrazine and doxorubicin hydrochloride. Notably, prodrugs **1**, **2**, and **3** formed monodispersed nanogels with average sizes of 114.4, 75.3, and 66.3 nm, respectively, in phosphate buffer (PB, 10 mM, pH 7.4). The *in vitro* release results showed that DOX was released rapidly and nearly quantitatively from DOX prodrug nanogels at endosomal pH and 37 °C in 48 h, whereas only a minor amount (ca. 20% or less) of drug was released at pH 7.4 under otherwise the same conditions. Confocal laser scanning microscope (CLSM) observations revealed that DOX prodrug nanogels delivered and released DOX into the cytosols as well as cell nuclei of RAW 264.7 cells following 24 h incubation. MTT assays demonstrated that prodrug **3** had pronounced cytotoxic effects to tumor cells following 72 h incubation with IC_{50} data determined to be 2.0 and 3.4 μg DOX equiv/mL for RAW 264.7 and MCF-7 tumor cells, respectively. The corresponding polymer carrier, PEG-*b*-P(HEMA-*co*-GMA-hydrazide), was shown to be nontoxic up to a tested concentration of 1.32 mg/mL. These endosomal pH-activatable DOX prodrug nanogels uniquely combining features of water-soluble macromolecular prodrugs and nanogels offer a promising platform for targeted cancer therapy.

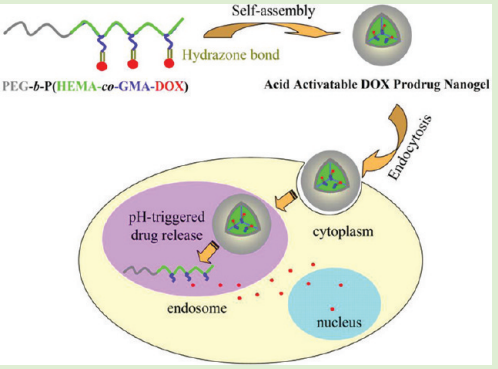

INTRODUCTION

In the past decades, polymeric prodrugs based on biocompatible water-soluble polymers such as poly(*N*-(2-hydroxypropyl)-methacrylamide) (PHPMA) and poly(ethylene glycol) (PEG) have received tremendous interest for targeted cancer therapy.[1−6] Unlike self-assembled nanovehicles including micelles and polymersomes that tend to dissociate and release encapsulated drug upon intravenous administration, polymeric prodrugs are much more stable and may effectively prevent premature drug release. In addition, polymeric prodrugs can increase water solubility of lipophilic drugs, protect drug from aggregation and/or degradation, and enhance drug bioavailability. Therefore, macromolecular prodrugs can on one hand improve the *in vivo* drug efficacy and on the other hand significantly reduce drug-associated side effects.[7] Notably, several macromolecular prodrugs have been approved for different phases of clinical trials.[8−10]

The current polymeric prodrugs are usually based on relatively low molecular weight (M_w < 45 kDa) water-soluble polymers because higher molecular weight PHPMA or PEG polymers cannot readily be excreted from the body.[8,11] The low molecular weight macromolecular drugs, however, exhibit relatively short circulation time and poor accumulation in the tumor *in vivo*.[3,12] In recent years, prodrug micelles with anticancer drug (e.g., DOX or paclitaxel) covalently conjugated to the micellar core via a cleavable hydrazone, amide, or ester bond, which elegantly combine stability of prodrugs and long circulation time of micelles, were actively developed for improved cancer therapy.[13] For example, Park and co-workers reported acid activatable micellar DOX prodrugs through conjugating DOX to PEG−PLA terminal via pH-sensitive hydrazone or *cis*-aconityl bond.[14] Kataoka and co-workers prepared environment-sensitive micellar prodrugs from PEG−polyaspartate block copolymer grafted with DOX via a hydrazone linkage.[15−17] Ulbrich and co-workers reported that pH-sensitive DOX prodrug micelles with DOX covalently conjugated to the PEO-*b*-PAGE micelle core via a hydrazone bond had reduced systemic toxicity and pronounced

Received: June 27, 2011
Revised: September 7, 2011
Published: September 9, 2011

Scheme 1. Illustration on Acid-Activatable DOX Prodrug Nanogels That Selectively Release DOX at Endosomal Compartments

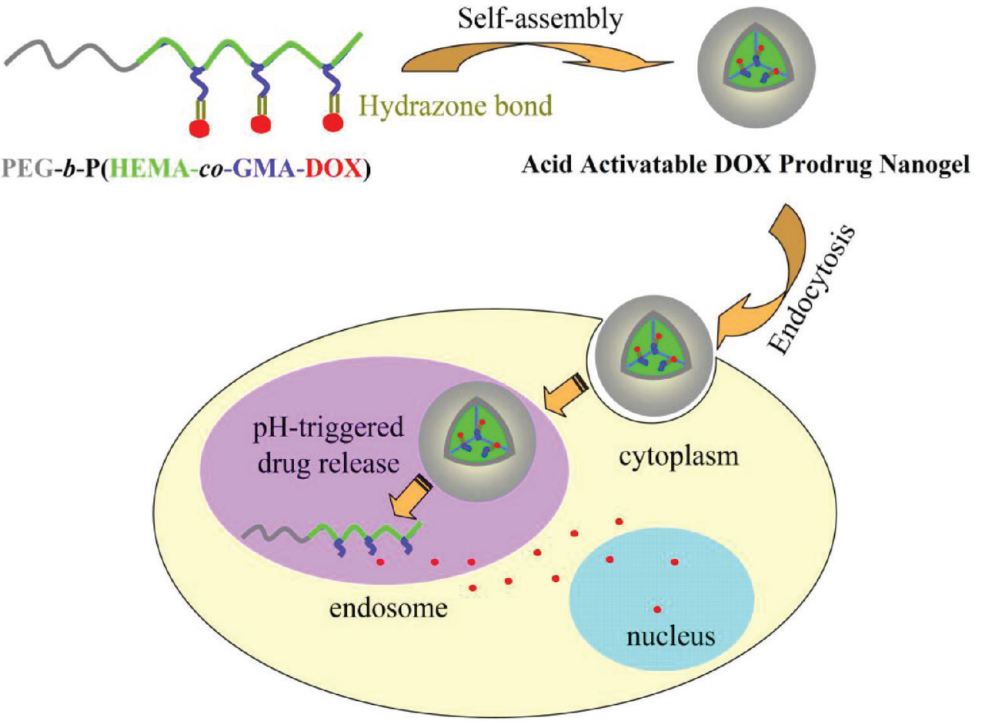

therapeutic activity in murine EL-4 T-cell lymphoma-bearing mice.[18,19] Jing and co-workers prepared paclitaxel (PTX) prodrug micelles by conjugating PTX to biodegradable amphiphilic block copolymer via an ester bond and tumor-targeting DOX prodrug micelles via a carbamate or hydrazone linkage.[20,21] It should be noted, nevertheless, that drug release from prodrug micelles are often slow and incomplete (e.g., less than 50% even after several days) likely due to retarded hydrolysis and drug diffusion within the hydrophobic micellar core.

In this paper, we report on novel endosomal pH-activatable DOX prodrug nanogels based on poly(ethylene glycol)-*b*-poly(2-hydroxyethyl methacrylate-*co*-glycine methacrylamide-DOX) (PEG-*b*-P(HEMA-*co*-GMA-DOX)) (Scheme 1). DOX was grafted to the macromolecular carrier via an acid-labile hydrazone bond, which is known to be sufficiently stable at pH 7.4 but readily cleavable at endosomal pH.[14,15,21,22] Notably, prodrug nanogels could be obtained via directly dispersing DOX prodrugs in aqueous media, which not only avoids use of (toxic) organic solvents but also largely simplifies production and handling. The formation of nanogels is driven by hydrophobic interactions between conjugated DOX. The stimuli-responsive activation and release of drug from prodrug nanogels could take place rapidly, likely due to the fact that nanogels have excellent permeability.[23−25] The polymer precursor was based on PEG, PHEMA, and glycine that are widely used for biomedical applications. Herein, synthesis of DOX prodrugs, pH-dependent drug release from DOX prodrug nanogels, intracellular release of DOX, and *in vitro* cytotoxicity of DOX prodrug nanogels were investigated.

EXPERIMENTAL SECTION

Materials. Methoxy poly(ethylene glycol) (PEG, M_n = 5.0 kg/mol, Fluka) was dried by azeotropic distillation from toluene. Methanol, dichloromethane (DCM), dimethylformamide (DMF), 2,2′-azobis-(isobutyronitrile) (AIBN), doxorubicin hydrochloride (DOX·HCl, >99%, Beijing ZhongShuo Pharmaceutical Technology Development Co., Ltd.), hydrazine hydrate aqueous solution (85%, Sinopharm Chemical Reagent), ethyl glycinate hydrochloride (99.5%, Sinopharm Chemical Reagent), methacryloyl chloride (Wuxi Chemical), acetic acid (99.5%, Sinopharm Chemical Reagent), and trifluoroacetic anhydride (TFA, 99%, Alfa-Aesar) were used as received. 2-Hydro xyethyl methacrylate (HEMA) was purified as reported.[26] PEG-CPADN was synthesized similar to our previous report for CPADN-PCL-CPADN.[27]

Synthesis of Ethyl Glycinate Methacrylamide (EGMA). To an aqueous solution (20 mL) of ethyl glycinate hydrochloride (5.0 g, 0.036 mol) at 0 °C were added dropwise a DCM solution (5 mL) of methacryloyl chloride (3.78 g, 0.036 mol) and an aqueous NaOH solution (7.2 mM, 10 mL) simultaneously. The reaction was warmed to room temperature (rt) and allowed to proceed for an additional 5 h after completion of addition. The organic layer was purified by silica gel column chromatography (eluent: petroleum ether/ethyl acetate 1/2 v/v). Then, the product was concentrated and dried in vacuo. Yield: 71.2%. ^{1}H NMR (400 MHz, DMSO-d_6): δ 1.19 (m, 3H), 4.06 (m, 2H), 3.81 (d, 2H), 8.35 (s, 1H), 1.87 (s, 3H), 5.39 (s, 1H), 5.71 (s, 1H).

Synthesis of PEG-*b*-P(HEMA-*co*-EGMA) by RAFT Polymerization. PEG-*b*-P(HEMA-*co*-EGMA) copolymers were prepared by RAFT polymerization of HEMA and EGMA using PEG-CPADN as a macro-RAFT agent. In a typical example, under a nitrogen atmosphere, HEMA (73 μL, 606 μmol), EGMA (21.0 mg, 123 μmol), AIBN (0.48 mg, 3.0 μmol), PEG-CPADN (10.0 mg, 2.0 μmol), and methanol/DMF (6/1, v/v, 1.4 mL) were added into a 10 mL Schlenk flask. The flask was sealed and placed in an oil bath thermostated at 50 °C. The polymerization proceeded with stirring for 48 h. The resulting copolymer was isolated by precipitation in cold diethyl ether, filtration, and drying in vacuo. Yield: 72−85%. ^{1}H NMR (400 MHz, DMSO-d_6): δ 0.61−1.04 (m, −CC**H**$_3$, HEMA; −CC**H**$_3$, EGMA), 1.18 (m, −CH$_2$C**H**$_3$, EGMA), 1.65 −2.02 (s, −CC**H**$_2$−, HEMA; −CC**H**$_2$−, EGMA), 3.50 (s, PEG), 3.58 (m, −C**H**$_2$OH, HEMA), 3.88 (m, −COOC**H**$_2$−, HEMA; −NHC**H**$_2$COO−, EGMA), 4.05 (m, −COOC**H**$_2$−, EGMA), 4.83 (s, −CH$_2$O**H**, HEMA).

Synthesis of PEG-*b*-P(HEMA-*co*-GMA-hydrazide). To a 25 mL Schlenk flask equipped with a magnetic stirrer were added PEG-*b*-P(HEMA-*co*-EGMA) (100 mg, 55 μmol COOCH$_2$CH$_3$), hydrazine hydrate (31 μL, 639 μmol), and anhydrous methanol (2 mL).

dx.doi.org/10.1021/bm200876x|*Biomacromolecules* 2011, 12, 3612−3620

The flask was sealed, and the reaction was allowed to proceed for 10 h at rt. The polymer precursor was isolated by extensive dialysis (MWCO 3500) against DI water and freeze-drying. Yield: 80 mg (80%). The content of hydrazide was determined by modified TNBSA assays as described by Ulbrich and co-workers.[28]

Synthesis of PEG-*b*-P(HEMA-*co*-GMA-DOX) Prodrugs. In a typical example, to a 25 mL Schlenk flask equipped with a magnetic stirrer were added PEG-*b*-P(HEMA-*co*-GMA-hydrazide) (76.0 mg, 39 μmol of hydrazide), doxorubicin hydrochloride (44.1 mg, 76 μmol), a drop of acetic acid, and anhydrous methanol (2 mL). The flask was sealed, and the reaction was allowed to proceed in the dark for 48 h at rt. The prodrug was isolated by extensive dialysis against anhydrous methanol (MWCO 3500) followed by dialysis against DI water and lyophilization. Yield: 78 mg (78%). To determine DOX content, 1.0 mg of prodrug was treated with 1 N HCl at rt for 24 h. The resulting solution was diluted with DI water. The amount of free DOX was determined using fluorescence spectroscopy at the emission wavelength of 560 nm, excitation wavelength of 480 nm, and the width of 5 nm. The calibration curve was prepared using DOX·HCl solution in DI water. The free DOX content was determined by dissolving 1.0 mg of prodrug in anhydrous methanol and using extensive dialysis against anhydrous methanol (MWCO 3500). The DOX content remained in the dialysis tube was determined as described above. The results showed less than 0.2% loss of DOX, confirming a low amount of free drug in PEG-*b*-P(HEMA-*co*-GMA-DOX) conjugates.

Characterization. ^{1}H NMR spectra were recorded on a Unity Inova 400 spectrometer operating at 400 MHz using DMSO-d_6 as a solvent. The chemical shifts were calibrated against residual solvent signal. The polydispersity of copolymers were determined by a Waters 1515 gel permeation chromatograph (GPC) instrument equipped with a Styragel HR 5E column (M_w from 2000 to 4×10^6 g/mol) following a INLINE precolumn and a differential refractive index detector. The measurements were performed using tetrahydrofuran (THF) as an eluent at a flow rate of 0.5 mL/min at 35 °C and a series of narrow polystyrene as standards for the calibration of the columns. The size (hydrodynamic radius R_h) of nanogels was determined using dynamic light scattering (DLS). Measurements were carried out at 25 °C using Zetasizer Nano-ZS from Malvern Instruments equipped with a 633 nm He−Ne laser using backscattering detection. The fluorescence measurements of DOX were performed using an EDINBURGH FLS920 spectrofluorometer. Excitation and emission were set at 480 and 555 nm, respectively, with bandwidth of 5 nm.

Change of Nanogel Size in Time under Acidic Conditions. The size change of prodrug nanogel **3** under acidic condition (pH 5.0, 100 mM acetate buffer) was followed by DLS. Briefly, 2 mL of prodrug **3** nanogel dispersion (0.5 mg/mL) was dialyzed against acetate buffer (pH 5.0, 100 mM) at 37 °C. At the desired time points, an aliquot of 0.7 mL of solution in the dialysis tube was removed and measured by DLS.

***In Vitro* Drug Release.** The release of DOX from prodrugs **1**, **2**, and **3** was studied at 37 °C in three different media, that is, (a) acetate buffer, pH 5.0; (b) acetate buffer, pH 6.0; and (c) phosphate buffer, pH 7.4. In a typical experiment, 1.0 mg of prodrug was dissolved in 20 mL of water for about 10 min to obtain stable nanogels. An aliquot of 0.7 mL of solution was transferred to a dialysis tube with an MWCO of 3500. The dialysis tube was immersed in 30 mL of pH 5.0 acetate buffer, pH 6.0 acetate buffer, or pH 7.4 phosphate buffer (0.1 M) at 37 °C with constant shaking (200 rpm). At desired time intervals (i.e., 0.5, 1.5, 2.5, 4, 6, 8.5, 11.5, 22.5, 31.5, and 47 h), 6 mL of release media was taken out for fluorescence measurement and replenished with an equal volume of corresponding fresh media. DOX was determined using fluorescence spectroscopy at the emission wavelength of 560 nm, excitation wavelength of 480 nm, and the slit width of 5 nm. The release experiments were conducted in triplicate. The results presented are the average data.

Intracellular Release of DOX. The cellular uptake and intracellular release behavior of prodrug **3** were followed with confocal laser scanning microscopy (CLSM) using mouse leukemic monocyte macrophage cell line (RAW 264.7). RAW 264.7 cells were cultured in an 18 mm round disk placed in 24-well plates (5×10^4 cells/well) for 1 day. Then, prodrug **3** (40 μg DOX equiv/mL) was added, and cells were cultured for 6, 12, or 24 h in a humidified 5% CO_2-containing atmosphere. The culture media was removed, the cells after being rinsed two times with PBS were fixed with formaldehyde, and the cell nuclei were stained with 4′,6-diamidino-2-phenylindole (DAPI, blue). CLSM images of cells were obtained using confocal microscope (TCS SP2). The cells treated with free DOX (40 μg/mL) were used as a control.

MTT Assays. The cytotoxicity of prodrug **3** and corresponding polymer precursor was assessed by MTT assays. RAW 264.7 or MCF-7 cells were plated in a 96-well plate (5×10^3 cells/well) using RPMI 1640 medium for 1 day. The cells were incubated with prodrug **3** at varying concentrations of 0.1−10 μg of DOX equiv/mL, free DOX at varying concentrations of 0.1−10 μg/mL, or corresponding polymer precursor at concentrations ranging from 0.33 to 1.32 mg/mL for 72 h at 37 °C in a humidified 5% CO_2-containing atmosphere. The media was aspirated and replenished with 100 μL of fresh culture medium. A stock solution (20 μL) containing 0.1 mg of 3-(4,5-dimethylthiazol-2-yl)-2,5-diphenyltetrazolium bromide (MTT) in PBS was added, and the cells were incubated for another 4 h. The media was aspirated, the MTT-formazan generated by live cells was dissolved in 150 μL of DMSO, and the absorbance at a wavelength of 490 nm of each well was measured using a microplate reader. The relative cell viability (%) was determined by comparing the absorbance at 490 nm with control wells containing only cell culture medium. Data are presented as average ± SD (n = 3).

RESULTS AND DISCUSSION

Design and Synthesis of Endosomal pH-Activatable DOX Prodrug Nanogels. The aim of this study was to develop acid-activatable doxorubicin (DOX) prodrug nanogels that uniquely combine features of both prodrugs and nanogels; e.g., (i) they can directly and reproducibly be dispersed in aqueous media, thereby avoiding use of (toxic) organic solvents, (ii) while sufficiently stable at pH 7.4 they are able to rapidly release drug in response to endosomal pH environment, achieving selective and efficient intracellular drug release in tumor cells, and (iii) they have tunable particle sizes ranging from 20 to 150 nm, likely prolonging circulation time, improving tumor targetability, and enhancing intracellular drug release. To this end, DOX prodrugs, poly(ethylene glycol)-*b*-poly(2-hydroxyethyl methacrylate-*co*-glycine methacrylamide-DOX) (PEG-*b*-P(HEMA-*co*-GMA-DOX)) in which DOX was conjugated to the macromolecular carrier via an acid-sensitive hydrazone bond, were designed (Scheme 1). PHEMA was selected to form core of nanogels since it is a well-established biocompatible hydrogel forming polymer.[29,30] Here, to achieve controlled conjugation of DOX, a new α-amino acid-based monomer, ethyl glycinate methacrylamide (EGMA), was designed and prepared (Scheme 2). α-Amino acid has widely been used for development of functional biomaterials.[31] The ^{1}H NMR spectrum showed signals at δ 1.87, 5.39, and 5.71 attributable to the methacrylamide moieties, resonances at δ 1.19, 3.81, and 4.08 assignable to ethyl glycinate moieties, and a singlet at δ 8.35 due to the amide proton (Figure 1). Notably,

Scheme 2. Synthesis of Ethyl Glycinate Methacrylamide (EGMA)[a]

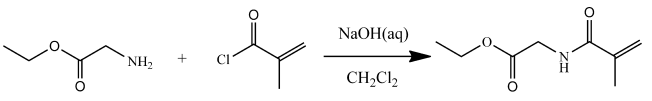

[a]Conditions: DI water/CH_2Cl_2 = 6/1 (v/v), 7.2 mM NaOH, 25 °C, 5 h.

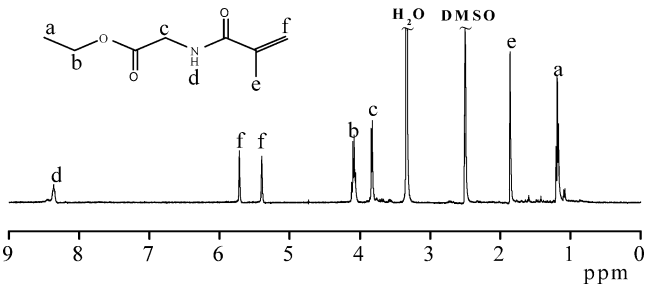

Figure 1. ^{1}H NMR spectrum (400 MHz, DMSO-d_6) of EGMA.

the signals at δ 5.39/5.71 (methylene protons of methacrylamide moieties) and δ 4.08 (methylene protons next to the ester bond of ethyl glycinate moieties) had an intensity ratio of close to 1:1, indicating equivalent coupling of ethyl glycinate and methacryloyl chloride.

The prodrugs were readily synthesized in three steps (Scheme 3). First, PEG-*b*-P(HEMA-*co*-EGMA) copolymers were prepared by radical addition−fragmentation chain transfer (RAFT) copolymerization of HEMA and EGMA using PEG-CPADN (CPADN: 4-cyanopentanoic acid dithionaphthalenoate) as a macro-RAFT agent and AIBN as the radical source in methanol/DMF (6/1 v/v) at 50 °C for 48 h. CPADN is a versatile RAFT agent, through which we have prepared structurally well-defined PDMAEMA−PCL−PDAMEMA and PEG−PCL−PDEAEMA triblock copolymers.[27,32] The resulting

Table 1. Synthesis of PEG-*b*-P(HEMA-*co*-EGMA) Copolymers by RAFT Copolymerization[a]

entry	f_{EGMA}[b]	F_{EGMA}[c]	M_n (^{1}H NMR)[d]	M_n (GPC)[e]	PDI[e]	yield (%)
1	10.3	10.5	5000−3100	8700	1.22	72
2	15.4	17.3	5000−3300	8600	1.20	75
3	20.5	21.1	5000−3500	9200	1.25	85

[a]The polymerization was carried out in methanol/DMF at 50 °C for 48 h in the presence of PEG-CPADN ($M_{n,PEG}$ = 5.0 kg/mol) and AIBN. The M_n of P(HEMA-*co*-EGMA) block was designed to be 5.0 kg/mol. [b]Mole feed ratio of EGMA. [c]Mole fraction of EGMA units in P(HEMA-*co*-EGMA) block determined by ^{1}H NMR. [d]Calculated by ^{1}H NMR. [e]Determined by GPC measurements (eluent: THF, flow rate: 0.5 mL/min, polystyrene standards).

Scheme 3. Synthesis of PEG-*b*-P(HEMA-*co*-GMA-DOX) Prodrugs[a]

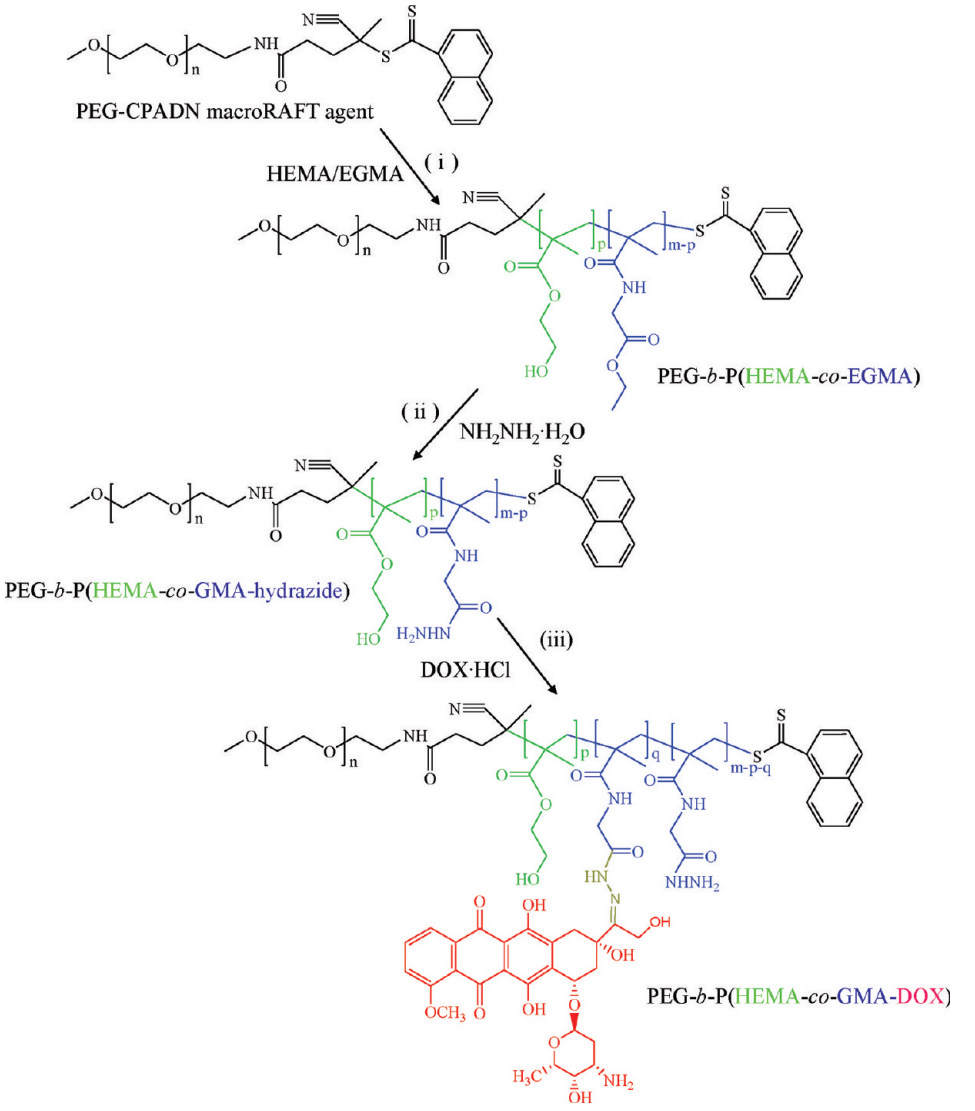

[a]Conditions: (i) AIBN, methanol/DMF, 50 °C, 48 h; (ii) methanol, 25 °C, 10 h; (iii) acetic acid, methanol, 25 °C, 48 h.

dx.doi.org/10.1021/bm200876x|*Biomacromolecules* 2011, 12, 3612−3620

block copolymers were isolated at 72−85% yields following precipitation from diethyl ether. The results of polymerization are shown in Table 1. ^{1}H NMR displayed clearly peaks characteristic of PEG block (δ 3.50), HEMA units (δ 3.56 and 4.83) and EGMA units (δ 1.18 and 4.05) (Figure 2A).

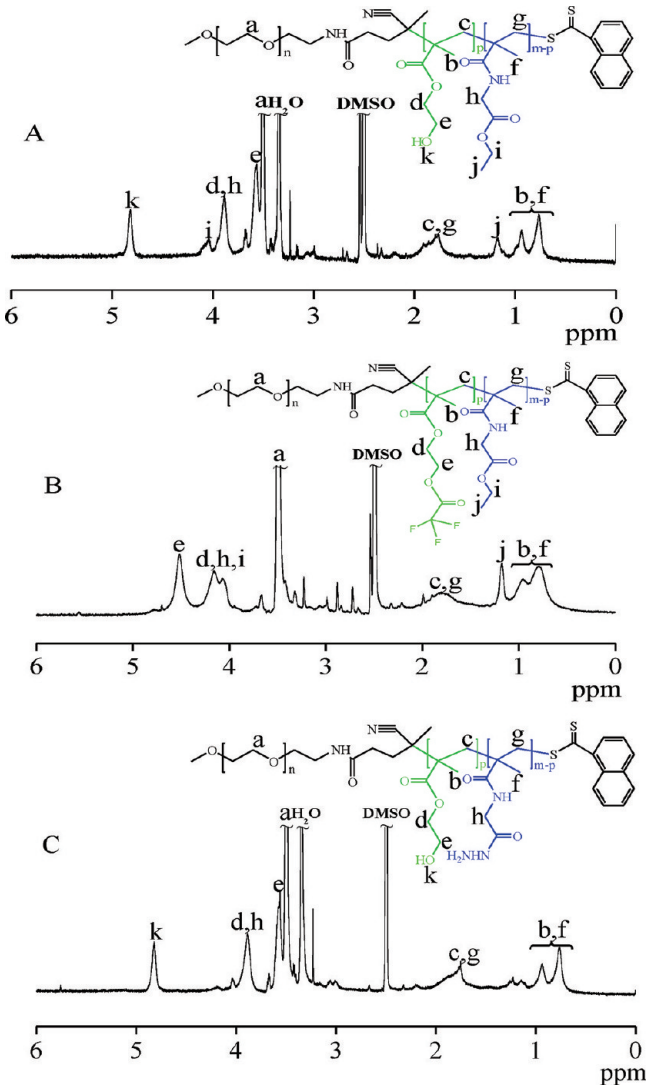

Figure 2. ^{1}H NMR spectra (400 MHz, DMSO-d_6) of PEG-*b*-P(HEMA-*co*-EGMA) (Table 1, entry 3) before (A) and after treating with trifluoroacetic anhydride (B) and PEG-*b*-P(HEMA-*co*-GMA-hydrazide) (Table 2, entry 3) (C).

The mole fractions of EGMA residue were calculated to be 10.5, 17.3 and 21.1% by comparing signals at δ 3.88 (−COOC**H**$_2$−, HEMA; −NHC**H**$_2$COO−, EGMA) and 4.05 (−COOC**H**$_2$−, EGMA) at EGMA mole feed fractions of 10.3, 15.4 and 20.5%, respectively (Table 1), indicating good control of copolymer compositions. To separate signals of PEG methylene protons from methylene protons next to the hydroxyl group of HEMA units, PEG-*b*-P(HEMA-*co*-EGMA) was treated with trifluoroacetic anhydride. The results showed disappearance of signal attributable to the hydroxyl proton of HEMA units and shifting of signal of methylene protons next to the hydroxyl group from 3.56 to 4.50 (Figure 2B). The M_n values of P(HEMA-*co*-EGMA) block varied from 3100 to 3500 (Table 1), as estimated by comparing the intensities of signals at δ 3.50 (methylene protons of PEG) and 4.50 (Figure 2B). Gel permeation chromatography (GPC) showed that these copolymers had molecular weights close to those determined from ^{1}H NMR analyses and low polydispersities of 1.20−1.25 (Table 1), indicating controlled synthesis of PEG-*b*-P(HEMA-*co*-EGMA) copolymers.

Second, PEG-*b*-P(HEMA-*co*-EGMA) copolymers with EGMA mole fractions of 10.5, 17.3, and 21.1% were treated with hydrazine hydrate in methanol for 10 h at rt, which yielded water-soluble PEG-*b*-P(HEMA-*co*-GMA-hydrazide) derivatives with 8.5, 15.0, and 18.5 mol % hydrazide (referred to as prepolymers **1**, **2**, and **3**), respectively, as determined by TNBSA assays (Table 2). The conversion of ethyl ester to hydrazide was about 80.9−87.7%. The occurrence of hydrazinolysis was further confirmed by ^{1}H NMR that displayed diminishing intensity of signal at δ 4.05 attributable to the ethyl protons of EGMA units (Figure 2C). Notably, GPC showed that copolymer molecular weights as well as polydispersities were not much altered by hydrazinolysis (Table 2). As revealed by dynamic light scattering (DLS), all three prepolymers existed as unimers with average sizes in the range of 5−11 nm in water (Figure 3A).

Finally, acid-labile PEG-*b*-P(HEMA-*co*-GMA-DOX) prodrugs were obtained by treating PEG-*b*-P(HEMA-*co*-GMA-hydrazide) derivatives with DOX·HCl in methanol. The level of DOX conjugation was determined by fluorescence measurements following treatment with 1 N HCl at rt for 24 h. The results showed that DOX prodrugs with drug loading contents of 3.9, 5.7, and 11.7 wt % (denoted as prodrugs **1**, **2**, and **3**, respectively) were obtained from PEG-*b*-P(HEMA-*co*-GMA-hydrazide) derivatives with 8.5, 15.0, and 18.5 mol % hydrazide, respectively (Table 2). Interestingly, these prodrugs were readily and reproducibly dispersible in phosphate buffer (PB, 10 mM, pH 7.4) at 25 °C to form monodispersed nanogels (Figure 3B). The nanogel sizes decreased from 114.4 to 66.3 nm with increasing DOX contents from 3.9 to 11.7 wt %. To further investigate influences of DOX loading on nanogel formation, prodrugs with DOX contents varying from 1.4 to 11.7 wt % were prepared from prepolymer **3**. DLS showed that nanogel sizes decreased with increasing DOX contents (Figure 4), supporting that hydrophobic DOX acts as an physical cross-linker for the formation of nanogels. Notably, the scattering intensities of prodrug nanogels increased almost

Table 2. Characteristics of PEG-*b*-P(HEMA-*co*-GMA-hydrazide) Conjugates and PEG-*b*-P(HEMA-*co*-GMA-DOX) Prodrugs

	PEG-*b*-P(HEMA-*co*-GMA-hydrazide)				PEG-*b*-P(HEMA-*co*-GMA-DOX)		
entry	M_n (GPC)[a]	PDI (GPC)[a]	hydrazide (mol %)[b]	conv (%)	DOX (wt %)[c]	size (nm)[d]	PDI[d]
1	8800	1.27	8.5	80.9	3.9	114.4	0.15
2	9500	1.31	15.0	86.7	5.7	75.3	0.27
3	8800	1.25	18.5	87.7	11.7	66.3	0.22

[a]Determined by GPC measurements (eluent: THF, flow rate: 0.5 mL/min, polystyrene standards). [b]Determined by TNBSA assays. [c]Determined by fluorescence measurement. [d]Determined using Zetasizer Nano-ZS (Malvern Instruments) at a nanogel concentration of 1.0 mg/mL in PB (10 mM, pH 7.4) at 25 °C.

dx.doi.org/10.1021/bm200876x|*Biomacromolecules* 2011, 12, 3612−3620

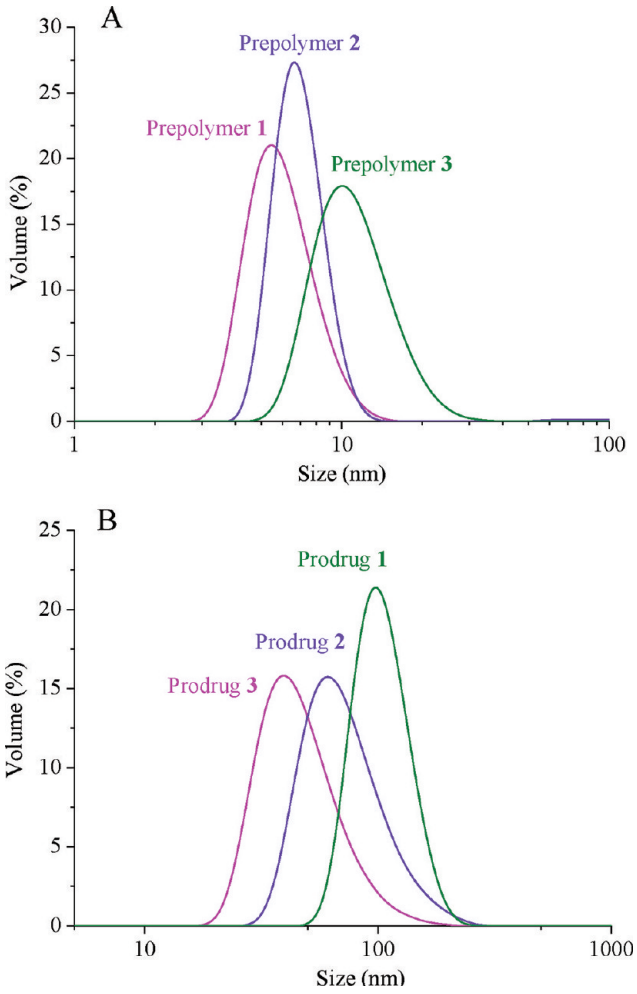

Figure 3. Size distributions of PEG-*b*-P(HEMA-*co*-GMA-hydrazide) prepolymers (A) and pH-activatable DOX prodrug nanogels (B) determined by DLS.

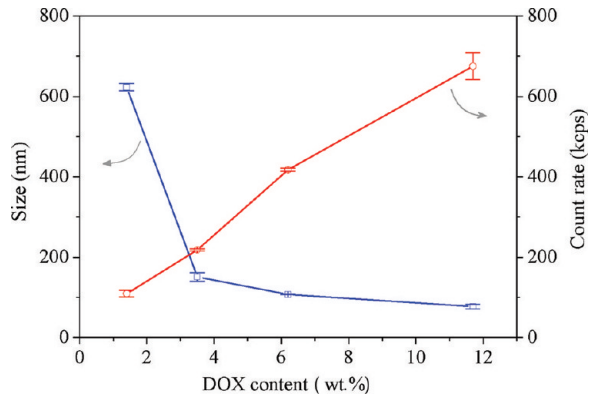

Figure 4. Influences of DOX contents on sizes and count rates of pH-activatable prodrug nanogels (0.2 mg/mL) based on prepolymer **3** determined by DLS.

proportionally to DOX contents (Figure 4), indicating that number of nanogels has increased significantly with increase of DOX loading.

***In Vitro* and Intracellular Drug Release.** The release of DOX from PEG-*b*-P(HEMA-*co*-GMA-DOX) prodrug nanogels was studied at three different conditions, i.e., pH 5.0, 6.0, and 7.4 at 37 °C. The results showed that drug release under mildly acidic environments was significantly faster than that at neutral pH (Figure 5). For example, approximately 64.0% and 87.4% of drug were released in 48 h at pH 6.0 and 5.0, respectively, from prodrug **1** (Figure 5A). In contrast, only 14.4% of drug was released at pH 7.4 under otherwise the same conditions. Very similar drug release profiles were also observed for prodrugs **2** and **3** (Figures 5B). For instance, 63.6% and 95.3% release of DOX were observed for prodrug **3** in 48 h at pH 6.0 and 5.0, respectively (Figure 5B). These results indicate that PEG-*b*-P(HEMA-*co*-GMA-DOX) prodrugs while sufficiently stable

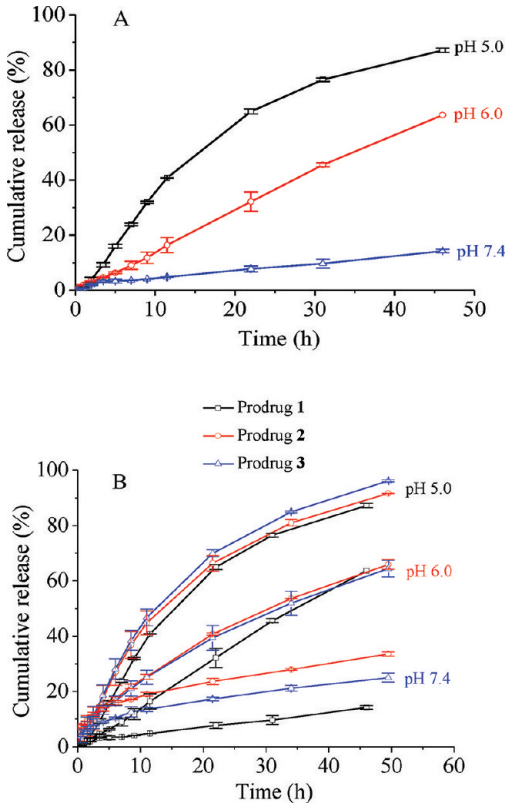

Figure 5. pH-dependent release of DOX at 37 °C from prodrug **1** (A) and prodrugs **1**, **2**, and **3** (B).

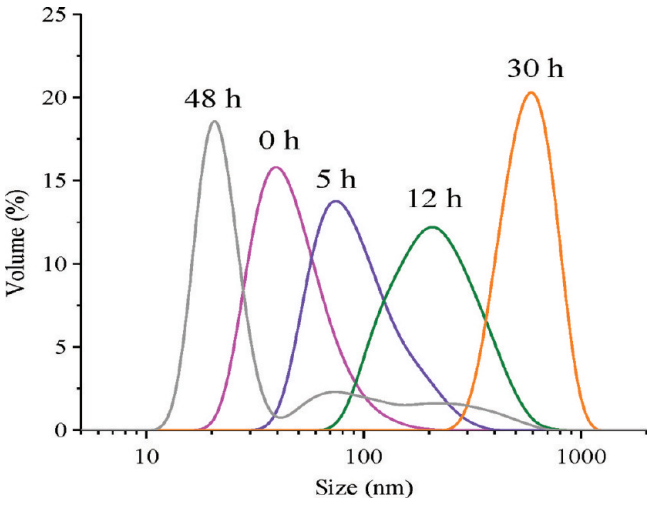

Figure 6. Change of size distributions of prodrug **3** nanogels at 37 °C and pH 5.0 (100 mM acetate buffer) in time monitored by DLS.

dx.doi.org/10.1021/bm200876x|*Biomacromolecules* 2011, 12, 3612–3620

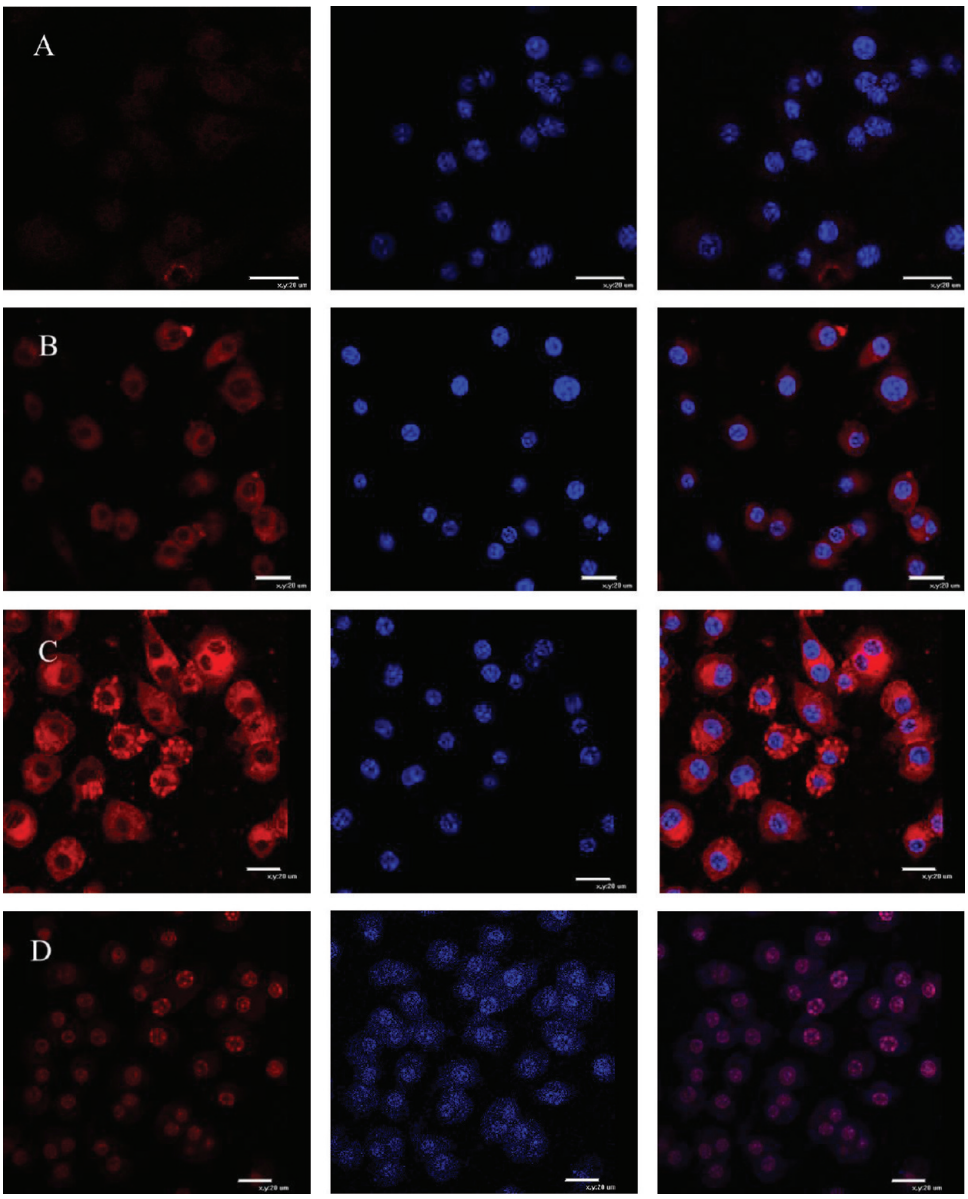

Figure 7. CLSM images of RAW 264.7 cells incubated with prodrug **3** and free DOX (40 μg equiv/mL). For each panel, the images from left to right show DOX fluorescence in cells (red), cell nuclei stained by DAPI (blue), and overlays of the two images. The scale bars correspond to 20 μm in all the images. (A) prodrug **3**, 6 h incubation; (B) prodrug **3**, 12 h incubation; (C) prodrug **3**, 24 h incubation; (D) free DOX, 6 h incubation.

under physiological conditions are likely quickly activable at endo/lysosomal compartments. Notably, these prodrug nanogels show similar pH-responsive drug release behaviors to water-soluble macromolecular DOX prodrugs,[33] which is likely due to their highly hydrophilic nature allowing excellent penetration of acid and fast diffusion of cleaved DOX. In comparison, DOX prodrug micelles with DOX covalently conjugated to the micelle core via a cleavable hydrazone bond were reported to exhibit slow and incomplete drug release even at acidic pH of 5.0. For example, Kataoka and co-workers reported that less than 30% of DOX was released from PEG-*b*-poly(aspartate-hydrazone-DOX) micelles in 72 h at pH 5.0.[15] Hrubý, Koňák, and Ulbrich reported that ~48% DOX was released in 380 h at pH 5.0 from DOX prodrug micelle based on PEO-*b*-PAGE block copolymer.[18] The drug release level would be further decreased at a higher DOX loading.[19] The slow drug release from prodrug micelles is most likely because hydrophobic micellar core presents a physical barrier for diffusion of acid into as well as cleaved DOX out of micelles. Therefore, acid-activatable prodrug nanogels have obvious advantages, i.e., enhanced pH sensitivity and superior drug release behaviors, over their micellar counterparts.

To investigate influences of DOX release on nanogel sizes, the size change of prodrug **3** nanogels was monitored in time at pH 5.0 (100 mM acetate buffer) and 37 °C by DLS. The results showed that nanogel sizes increased steadily to over 600 nm in 30 h and then decreased to ca. 20 nm in 48 h (Figure 6). These results are in accordance with previous observations that nanogel sizes increased with decreasing DOX contents. The nanogels would eventually fall apart when all DOX was cleaved off.

To investigate the intracellular drug release, DOX fluorescence in mouse leukemic monocyte macrophage cell line (RAW 264.7) was monitored by confocal laser scanning microscopy (CLSM). No DOX fluorescence was observed in RAW 264.7 cells following 6 h incubation with prodrug **3** (Figure 7A). However, after longer incubation time (e.g., 12

and 24 h), DOX was distributed to the whole cells including perinuclei and nuclei of RAW 264.7 cells (Figure 7B,C). DOX, one of the most potent anticancer drugs used widely in the treatment of different types of solid malignant tumors,[34] is known to exert drug effects via intercalation with DNA and inhibition of macromolecular biosynthesis.[35,36] It should be noted that free DOX was trafficked to the cell nuclei in 6 h (Figure 7D). Our previous results showed that under similar conditions PEG-*g*-DOX macromolecular prodrugs linked via a hydrazone bond displayed a faster intracellular release of DOX.[33] The slower intracellular DOX release from prodrug nanogels as compared to macromolecular prodrugs is most probably due to their reduced cellular uptake resulting from stealth effect of PEG shells. It is likely that for PEG-*g*-DOX prodrugs partially stealthed DOX would still facilitate non-specific endocytosis via e.g. hydrophobic interactions. DOX prodrug nanogels with superior stealth effect and desired particle sizes might provide a promising platform for prolonged circulation as well as tumor-targeted drug delivery via the enhanced permeability and retention (EPR) effect and/or installing an "active" targeting ligand.

***In Vitro* Cytotoxicity Studies.** The cytotoxicity of prodrug **3** and corresponding polymer carrier, i.e., PEG-*b*-P(HEMA-*co*-GMA-hydrazide), was investigated in RAW 264.7 and MCF-7 (human breast adenocarcinoma) cells by MTT assays. In the following studies, prodrug **3** was selected owing to its optimal drug loading and particle sizes. The cells were incubated with prodrug nanogels or polymer carrier for 72 h. The results revealed that PEG-*b*-P(HEMA-*co*-GMA-hydrazide) was non-toxic to both RAW 264.7 and MCF-7 cells at a tested concentration of up to 1.32 mg/mL (Figure 8), which corresponds

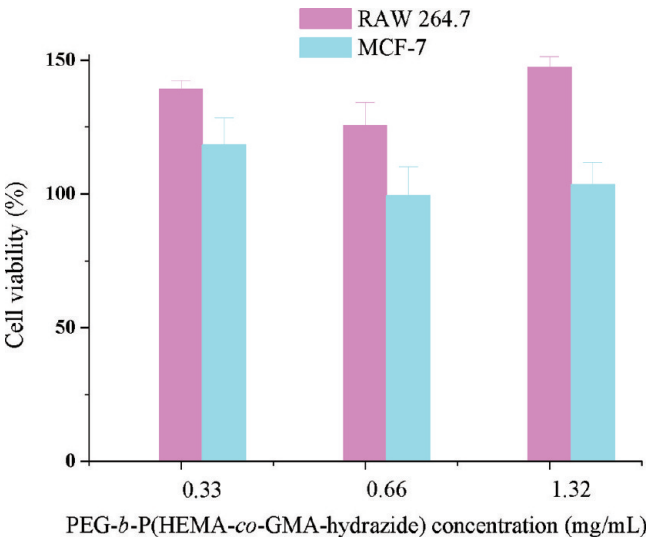

Figure 8. Cytotoxicity of PEG-*b*-P(HEMA-*co*-GMA-hydrazide) (Table 2, entry 3) at varying concentrations of 0.33, 0.66, and 1.32 mg/mL. RAW 264.7 and MCF-7 tumor cells were incubated with PEG-*b*-P(HEMA-*co*-GMA-hydrazide) for 72 h. The cell viability was determined by MTT assay (n = 3).

to a concentration of 170 μg of DOX equiv/mL for prodrug **3**, indicating that PEG-*b*-P(HEMA-*co*-GMA-hydrazide) has excellent biocompatibility and low cytotoxicity. The cell viabilities of RAW 264.7 cells was higher than 100%, likely due to activation of macrophage activity by nanogels. However, under otherwise the same conditions, prodrug **3** showed pronounced cytotoxic effects (Figure 8). For example, significantly reduced cell viabilities of about 34.6% and 38.4% were observed at a prodrug concentration of 5 μg of DOX equiv/mL for RAW 264.7 and MCF-7 cells, respectively. At a higher prodrug concentration of 10 μg of DOX equiv/mL, cell viabilities of RAW 264.7 and MCF-7 breast tumor cells further decreased to about 19.0% and 27.7%, respectively. The IC_{50} (i.e., inhibitory concentration to produce 50% cell death) values of prodrug **3** were determined to be 2.0 and 3.4 μg of DOX equiv/mL for RAW 264.7 and MCF-7 cells, respectively (Figure 9).

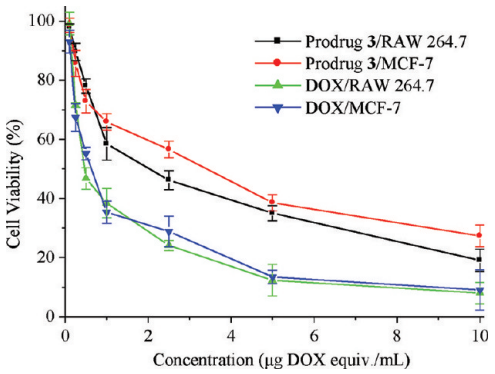

Figure 9. Cytotoxicity of prodrug **3** and free DOX at varying concentrations of 0.1−10 μg of DOX equiv/mL. RAW 264.7 and MCF-7 tumor cells were incubated with prodrug **3** or DOX for 72 h. The cell viability was determined by MTT assay (n = 3).

As commonly observed for polymeric prodrugs,[37−39] prodrug **3** was less toxic than free DOX *in vitro* that revealed IC_{50} data of 0.45 and 0.63 μg/mL for RAW 264.7 and MCF-7 breast tumor cells, respectively (Figure 9). This is likely because DOX prodrug nanogels have markedly reduced cellular uptake as compared to free DOX and furthermore prodrug has to be activated in endosomal compartments to exert the cytostatic effects. As revealed by CLSM studies, considerably longer time is needed for prodrug **3** to deliver DOX into the cell nuclei than direct application of free drug (Figure 7). It should be noted, however, that prodrug **3** has significantly lower IC_{50} as compared to PEG-*g*-DOX prodrugs (IC_{50} = 26.5−42.5 μg of DOX equiv/mL).[33] We observed that prodrug **3** though exhibiting slower cellular uptake than PEG-*g*-DOX prodrugs displayed much stronger DOX fluorescence in RAW 264.7 cells after prolonged incubation time (e.g., 24 h). In addition, cytotoxicity of prodrug nanogels to tumor cells might be significantly enhanced by installing a tumor-targeting ligand that facilitates specific cellular uptake.

CONCLUSIONS

We have demonstrated for the first time that endosomal pH-activatable DOX prodrug nanogels can readily be prepared from poly(ethylene glycol)-*b*-poly(2-hydroxyethyl methacrylate-*co*-glycine methacrylamide-DOX) (PEG-*b*-P(HEMA-*co*-GMA-DOX)) conjugates. These prodrug nanogels have uniquely combined advantages of macromolecular prodrugs and nanogels. On one hand, just like macromolecular prodrugs, they are directly and reproducibly dispersible in aqueous conditions, they are sufficiently stable with minimal drug release at neutral pH, and they achieve fast and complete drug release under mildly acidic conditions or inside cells. On the other hand, similar to nanogels, they have optimal particle sizes of tens to hundred nanometers as well as superior stealth surface

dx.doi.org/10.1021/bm200876x|*Biomacromolecules* 2011, 12, 3612−3620

that may lead to prolonged circulation time and enhanced accumulation in tumor. Notably, these DOX prodrug nanogels exhibit great cytotoxic effects to RAW 264.7 and MCF-7 tumor cells, which have about 1 order of magnitude lower IC_{50} as compared to their macromolecular prodrug counterparts. Importantly, corresponding polymer carrier, PEG-*b*-P(HEMA-*co*-GMA-hydrazide), is nontoxic up to a tested concentration of 1.32 mg/mL. These DOX prodrug nanogels have high potentials for the development of tumor-targeted drug delivery systems.

AUTHOR INFORMATION

Corresponding Author

*Tel: +86-512-65880098. E-mail: zyzhong@suda.edu.cn.

ACKNOWLEDGMENTS

This work was supported by National Natural Science Foundation of China (NSFC 20874070, 50973078, 20974073, 51003070, and 51173126), a Project Funded by the Priority Academic Program Development of Jiangsu Higher Education Institutions, and Program of Innovative Research Team of Soochow University.

REFERENCES

(1) Khandare, J.; Minko, T. *Prog. Polym. Sci.* **2006**, *31*, 359−397.
(2) Vicent, M. J.; Duncan, R. *Trends Biotechnol.* **2006**, *24*, 39−47.
(3) Kopecek, J.; Kopeckov, P. *Adv. Drug Delivery Rev.* **2010**, *62*, 122−149.
(4) Ulbrich, K.; Subr, V. *Adv. Drug Delivery Rev.* **2010**, *62*, 150−166.
(5) Duncan, R. *Nat. Rev. Cancer* **2006**, *6*, 688−701.
(6) Kopecek, J.; Kopeckova, P.; Minko, T.; Lu, Z. R. *Eur. J. Pharm. Biopharm.* **2000**, *50*, 61−81.
(7) Nori, A.; Kopecek, J. *Adv. Drug Delivery Rev.* **2005**, *57*, 609−636.
(8) Duncan, R. *Nat. Rev. Drug Discovery* **2003**, *2*, 347−360.
(9) Li, C.; Wallace, S. *Adv. Drug Delivery Rev.* **2008**, *60*, 886−898.
(10) Kratz, F.; Abu Ajaj, K.; Warnecke, A. *Expert Opin. Invest. Drugs* **2007**, *16*, 1037−1058.
(11) Fox, M. E.; Szoka, F. C.; Frechet, J. M. J. *Acc. Chem. Res.* **2009**, *42*, 1141−1151.
(12) Seymour, L.W.; Miyamoto, Y.; Maeda, H.; Brereton, M.; Strohalm, J.; Ulbrich, K.; Duncan, R. *Eur. J. Cancer* **1995**, *31*, 766−770.
(13) Hu, X. L.; Jing, X. B. *Expert Opin. Drug Delivery* **2009**, *6*, 1079−1090.
(14) Yoo, H. S.; Lee, E. A.; Park, T. G. *J. Controlled Release* **2002**, *82*, 17−27.
(15) Bae, Y.; Fukushima, S.; Harada, A.; Kataoka, K. *Angew. Chem., Int. Ed.* **2003**, *42*, 4640−4643.
(16) Bae, Y.; Nishiyama, N.; Fukushima, S.; Koyama, H.; Yasuhiro, M.; Kataoka, K. *Bioconjugate Chem.* **2005**, *16*, 122−130.
(17) Bae, Y.; Nishiyama, N.; Kataoka, K. *Bioconjugate Chem.* **2007**, *18*, 1131−1139.
(18) Hruby, M.; Konak, C.; Ulbrich, K. *J. Controlled Release* **2005**, *103*, 137−148.
(19) Vetvicka, D.; Hruby, M.; Hovorka, O.; Etrych, T.; Vetrik, M.; Kovar, L.; Kovar, M.; Ulbrich, K.; Rihova, B. *Bioconjugate Chem.* **2009**, *20*, 2090−2097.
(20) Xie, Z.; Guan, H. L.; Chen, X.; Lu, C.; Chen, L.; Hu, X.; Shi, Q.; Jing, X. *J. Controlled Release* **2007**, *117*, 210−216.
(21) Hu, X. L.; Liu, S.; Huang, Y. B.; Chen, X. S.; Jing, X. B. *Biomacromolecules* **2010**, *11*, 2094−2102.
(22) Lee, C. C.; Gillies, E. R.; Fox, M. E.; Guillaudeu, S. J.; Frechet, J. M. J.; Dy, E. E.; Szoka, F. C. *Proc. Natl. Acad. Sci. U. S. A.* **2006**, *103*, 16649−16654.
(23) Kabanov, A. V.; Vinogradov, S. V. *Angew. Chem., Int. Ed.* **2009**, *48*, 5418−5429.
(24) Raemdonck, K.; Demeester, J.; De Smedt, S. *Soft Matter* **2009**, *5*, 707−715.
(25) Oh, J. K.; Drumright, R.; Siegwart, D. J.; Matyjaszewski, K. *Prog. Polym. Sci.* **2008**, *33*, 448−477.
(26) Bajpai, A. K. *Polym. Int.* **2007**, *56*, 231−244.
(27) Zhu, C. H.; Jung, S.; Luo, S. B.; Meng, F. H.; Zhu, X. L.; Park, T. G.; Zhong, Z. Y. *Biomaterials* **2010**, *31*, 2408−2416.
(28) Etrych, T.; Jelinkova, M.; Rihova, B.; Ulbrich, K. *J. Controlled Release* **2001**, *73*, 89−102.
(29) Holly, F. J.; Refojo, M. F. *J. Biomed. Mater. Res.* **1975**, *9*, 315−326.
(30) Hoffman, A. S. *Adv. Drug Delivery Rev.* **2002**, *54*, 3−12.
(31) Sun, H.; Meng, F.; Dias, A. A.; Hendriks, M.; Feijen, J.; Zhong, Z. *Biomacromolecules* **2011**, *12*, 1937−1955.
(32) Liu, G. J.; Ma, S. B.; Li, S. K.; Cheng, R.; Meng, F. H.; Liu, H. Y.; Zhong, Z. Y. *Biomaterials* **2010**, *31*, 7575−7585.
(33) Zhou, L.; Cheng, R.; Tao, H.; Ma, S.; Guo, W.; Meng, F.; Liu, H.; Liu, Z.; Zhong, Z. *Biomacromolecules* **2011**, *12*, 1460−1467.
(34) Hortobagyi, G. N. *Drugs* **1997**, *54*, 1−7.
(35) Gewirtz, D. A. *Biochem. Pharmacol.* **1999**, *57*, 727−741.
(36) Tewey, K. M.; Rowe, T. C.; Yang, L.; Halligan, B. D.; Liu, L. F. *Science* **1984**, *226*, 466−468.
(37) Vaikunth Cuchelkar, P. K.; Kopecek, J. *Macromol. Biosci.* **2008**, *8*, 375−383.
(38) Ulbrich, K.; Etrych, T.; Chytil, P.; Jelinkova, M.; Rihova, B. *J. Controlled Release* **2003**, *87*, 33−47.
(39) Veronese, F. M.; Pasut, G. *Drug Discovery Today* **2005**, *10*, 1451−1458.